Molecular Therapy
Nucleic Acids
Original Article

LINC01234/MicroRNA-31-5p/MAGEA3 Axis Mediates the Proliferation and Chemoresistance of Hepatocellular Carcinoma Cells

Yunhao Chen,[1,2] Hui Zhao,[1,2] Haibo Li,[1,2] Xiao Feng,[1] Hui Tang,[1] Jianwen Zhang,[1] Binsheng Fu,[1] and Chunhui Qiu[1]

[1]Department of Hepatic Surgery, Liver Transplantation Center, The Third Affiliated Hospital of Sun Yat-Sen University, Guangzhou 510630, P.R. China

Hepatocellular carcinoma (HCC) is a prevalent malignancy characterized by aggressiveness and poor prognosis; however, the molecular mechanism remains to be fully identified. Based on the analysis of The Cancer Genome Atlas (TCGA) database, melanoma-associated antigen A3 (MAGEA3) and long non-coding RNA (lncRNA) LINC01234 were upregulated in HCC and associated with poor prognosis of HCC. We investigated the mechanism of how MAGEA3 and LINC01234 influenced HCC cellular functions and cisplatin resistance. MAGEA3 depletion inhibited proliferation, invasion, and cisplatin resistance of HepG2 cells and Huh7 cells *in vitro*, reduced resistance-associated protein 2 (MRP2), MRP3, and multidrug resistance protein 1 (MDR-1) expression, and elevated ALB expression. RNA pull-down and RIP assays identified the binding of LINC01234 and MAGEA3 to microRNA-31-5p (miR-31-5p). LINC01234 could restore MAGEA3 expression by binding to miR-31-5p. Furthermore, we delivered plasmids into HepG2 cells and Huh7 cells to alter the expression of LINC01234 and miR-31-5p. When miR-31-5p was downregulated, the proliferation and invasion of HepG2 cells and Huh7 cells were enhanced and the cisplatin-induced apoptosis was inhibited, while LINC01234 knockdown could diminish the effects caused by miR-31-5p depletion. In summary, these data highlight the vital role of MAGEA3/LINC01234/miR-31-5p axis in the HCC progression and chemoresistance of HCC cells.

INTRODUCTION

Liver cancer is a leading cause of cancer-related mortality,[1] and hepatocellular carcinoma (HCC) accounts for over 80% of all cases.[2] Particularly, approximately half of HCC cases occur in China.[3] Cisplatin-based chemotherapy has been widely used for HCC treatment.[4] However, many HCC patients displayed a negative response after chemotherapy due to the acquisition of drug resistance.[5] Besides, the postoperative living quality of HCC patients is not satisfying, despite the recent advancements in HCC treatment, including surgical resection, transplantation, radiofrequency, and chemotherapy.[6,7] Therefore, it is crucial to further explore the underlying mechanisms of progression and chemoresistance of HCC.

It has been recently demonstrated that the melanoma-associated antigen A (MAGEA) family is involved in cancer progression, including HCC, gastric cancer, and lung adenocarcinoma.[8–10] As a member of the MAGEA family situated in the X chromosome, MAGEA3 is widely known to be frequently and highly expressed in numerous cancers, including melanoma, lung, and ovarian cancer.[11] It was reported that MAGEA3 is closely correlated to poor clinical prognosis of non-small cell lung cancer patients, downregulation of which contributes to preventing cancer progression.[12] Moreover, through prediction by four databases, miRTarBase, microRNA.org, TargetScan, and mirDIP, it was found that MAGEA3 was highly expressed in HCC and could be targeted by microRNA-31-5p (miR-31-5p). On the other hand, miRs and long non-coding RNA (lncRNAs) have been identified to influence the properties and chemoresistance of cancer cells either directly or indirectly.[13] Restoration of miR-31-5p was shown to attenuate HCC cell growth, migration, and invasion.[14] Another study suggested that miR-31 downregulation weakens the chemoresistance of gallbladder cancer cells to cisplatin.[15] Moreover, lncRNAs can act to titrate miRNAs and thus restrain miRNA-mRNA binding.[16,17] For example, lncRNA LINC00066 has been found to play an oncogenic role in HCC by negatively modulating miR-214 expression.[18] LINC01234 has been previously highlighted as a prognostic biomarker predicting a low overall survival for ovarian cancer patients.[19] Bioinformatics prediction by the RNA22 website (https://cm.jefferson.edu/rna22/) revealed that lncRNA LINC01234 could bind to miR-31-5p.

Received 26 March 2019; accepted 28 October 2019;
https://doi.org/10.1016/j.omtn.2019.10.035.

[2]These authors contributed equally to this work.

Correspondence: Binsheng Fu, Department of Hepatic Surgery, Liver Transplantation Center, The Third Affiliated Hospital of Sun Yat-Sen University, No. 600, Tianhe Road, Tianhe District, Guangzhou 510630, Guangdong Province, P.R. China.
E-mail: fubinsh@mail.sysu.edu.cn
Correspondence: Jianwen Zhang, Department of Hepatic Surgery, Liver Transplantation Center, The Third Affiliated Hospital of Sun Yat-Sen University, No. 600, Tianhe Road, Tianhe District, Guangzhou 510630, Guangdong Province, P.R. China.
E-mail: zhjianw2@mail.sysu.edu.cn
Correspondence: Chunhui Qiu, Department of Hepatic Surgery, Liver Transplantation Center, The Third Affiliated Hospital of Sun Yat-Sen University, No. 600, Tianhe Road, Tianhe District, Guangzhou 510630, Guangdong Province, P.R. China.
E-mail: henryqiu@163.com

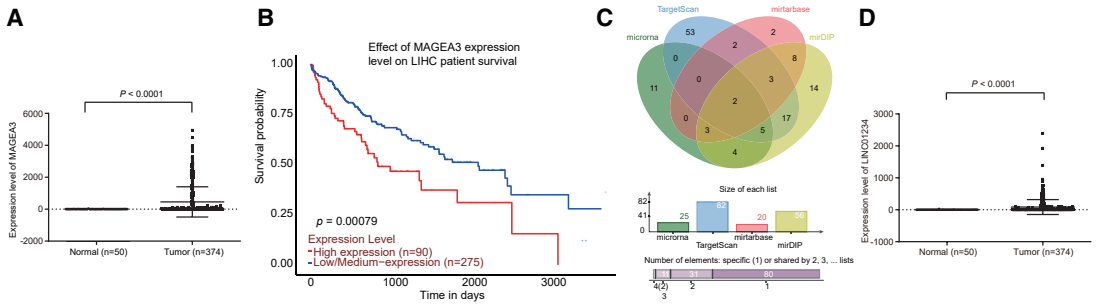

Figure 1. MAGEA3/LINC01234/miR-31-5p Axis Is Associated with the Development and Progression of HCC

(A) The expression of MAGEA3 in HCC and normal livers in TCGA database. (B) The relationship between MAGEA3 expression and survival time of HCC patients based on data analysis in TCGA database. (C) The predicted miRNAs targeting MAGEA3 in four databases (microRNA.org, targetscan.org, miRTarBase, and mirDIP online database). (D) The expression of LINC01234 in HCC and normal livers in TCGA database.

Hence, a hypothesis is proposed that LINC01234 might bind to miR-31-5p to regulate MAGEA3, which may be associated with the progression and chemoresistance of HCC. Thus, we sought to investigate the function and potential mechanism of LINC01234 in the progression and chemoresistance of HCC and determine the interaction among LINC01234, miR-31-5p, and MAGEA3 in these processes.

RESULTS

LINC01234/miR-31-5p/MAGEA3 Axis Is Involved in HCC

Initially, the gene-expressed profiles of 374 HCC and 50 normal livers in The Cancer Genome Atlas (TCGA) database were analyzed. The false discovery rate (FDR) < 0.05 and |log2 (fold change)| > 2 between both the HCC and normal tissue were set as the criteria to filter differentially expressed genes (DEGs). Expression of MAGEA3 was higher than that in the normal liver ($p < 0.0001$) (Figure 1A). As displayed in Figure 1B, a negative correlation was observed, and an elevated MAGEA3 expression often indicated poor prognosis of HCC ($p < 0.0001$). Next, we examined the potential miRNAs associated with MAGEA3, and miR-31-5p and miR-448 were predicated to be the possible miRNAs targeting MAGEA3 from miRTarBase (http://mirtarbase.mbc.nctu.edu.tw/php/search.php), microRNA.org (http://www.microrna.org/microrna/microrna/getMirnaForm.do), TargetScan (http://www.targetscan.org/vert_71/), and mirDIP (http://ophid.utoronto.ca/mirDIP/) (Figure 1C). Additionally, the RNA22 website (https://cm.jefferson.edu/rna22/) further predicted that LINC01234 could potentially bind to miR-31-5p. Expression of LINC01234 was higher in HCC compared with that in normal livers by TCGA database ($p < 0.0001$) (Figure 1D). Collectively, MAGEA3 and LINC01234 are highly expressed in HCC.

Downregulation of MAGEA3 Inhibits the Proliferation and Invasion but Promotes Apoptosis of HCC Cells

We sought to explore how MAGEA3 influences HCC cells and small interfering RNAs (siRNAs) targeting MAGEA3 (si-MAGEA3-1 and si-MAGEA3-2) were transfected into HepG2 cells. As shown in Figure 2A, the expression of MAGEA3 in HepG2 cells was suppressed upon si-MAGEA3-1 or si-MAGEA3-2 transfection. Therefore, si-MAGEA3-2 (si-MAGEA3) with the highest silencing efficiency in HepG2 cells was selected for subsequent use. Consistently, si-MAGEA3-2 in Huh7 cells also exhibited the highest silencing efficiency (Figure S1A). Then the viability of HepG2 cells and Huh7 cells was assessed using 3-(4,5-dimethylthiazol-2-yl)-2, 5-diphenyltetrazolium bromide (MTT) assay. Significant decreases in viability of HepG2 cells and that of Huh7 cells were detected at 24, 48, or 72 h after si-MAGEA3 transfection (Figure 2B; Figure S1B). Chemoresistance of HCC cells to cisplatin remains as a big challenge for the treatment of HCC.[20] In order to investigate the effects of MAGEA3 on HCC cell chemoresistance to cisplatin, we explored whether knocking down MAGEA3 could influence cisplatin-induced apoptosis of HepG2 cells and Huh7 cells using flow cytometry. As depicted in Figure 2C and Figure S1C, knocking down MAGEA3 potentiated apoptosis of HepG2 cells and Huh7 cells induced through low-concentration cisplatin (3 μg/mL) ($p < 0.05$). Additionally, we analyzed the effect of MAGEA3 on cell invasion. HepG2 cells and Huh7 cells were cultured in the Transwell chamber pre-coated with Matrigel. The results showed that the invasion of HepG2 cells and Huh7 cells was obviously attenuated upon the silence of MAGEA3 (Figure 2D; Figure S1D). Moreover, the protein expression of E-cadherin in HepG2 cells and Huh7 cells was measured by applying western blot analysis, which displayed that the protein expression of E-cadherin, was reduced in response to MAGEA3 depletion (Figure 2E; Figure S1E). Collectively, MAGEA3 might be oncogenic, and the knockdown of MAGEA3 could reduce proliferation and invasion while enhancing apoptosis of HepG2 cells and Huh7 cells.

MAGEA3 Depletion Attenuates Chemoresistance of HCC Cells to Cisplatin

To assess the effects of MAGEA3 silencing on chemoresistance of HCC cells to cisplatin, HepG2 cells and Huh7 cells were transfected with siRNAs and treated with various concentrations of cisplatin (0, 2.5, 5, 10, 20, and 40 μg/mL) for 48 consecutive h. A cell counting kit-8 (CCK-8) assay revealed that the 50% inhibitive concentration (IC_{50}) of mock HepG2 cells and siRNA-negative control (si-NC)-transfected HepG2 cells was 13.6 μg/mL, which was relatively higher in comparison to the HepG2 cells transfected with si-MAGEA3 (5.3 μg/mL). This indicated that the IC_{50} of HepG2 cells was reduced in response to MAGEA3

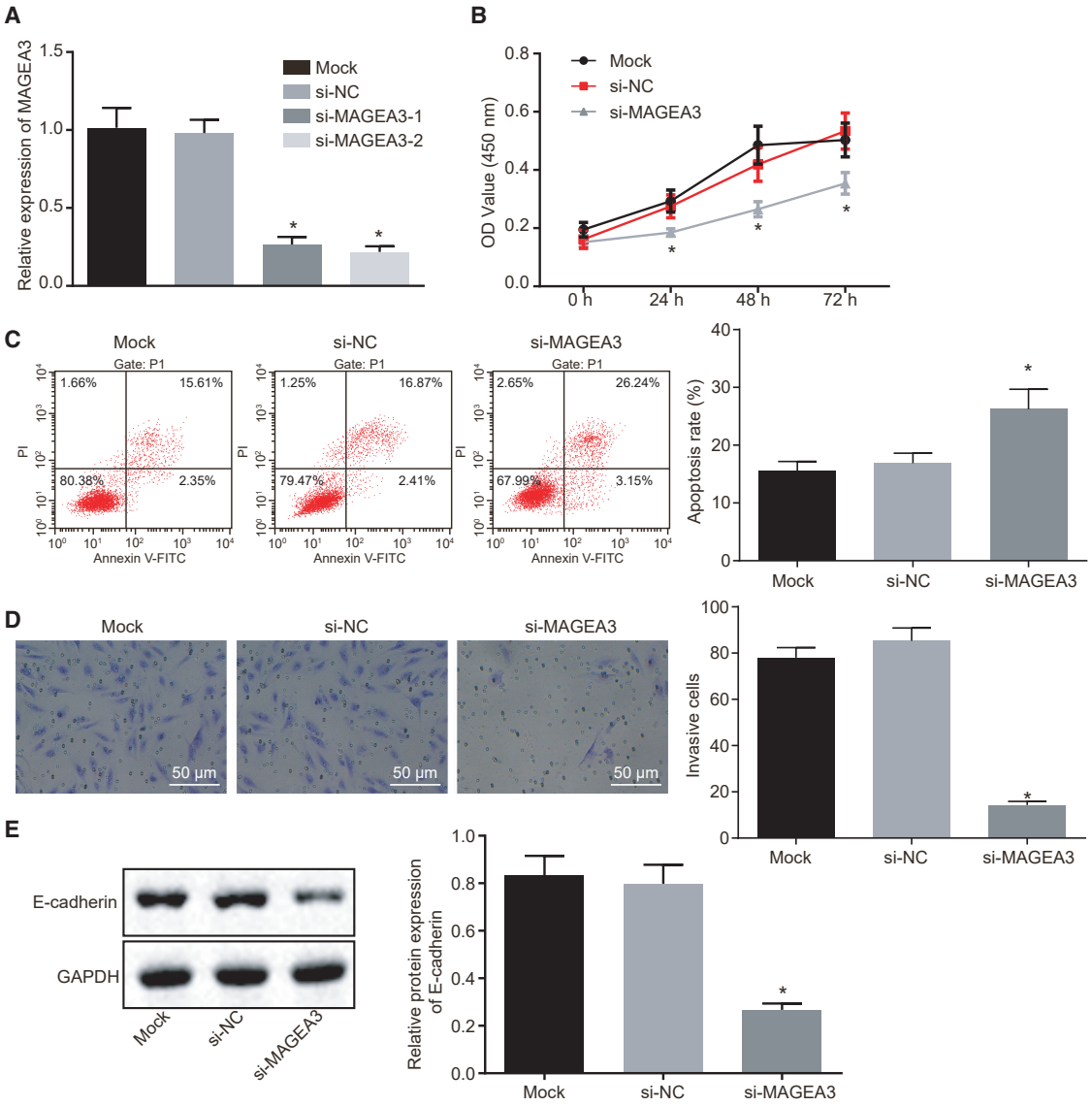

Figure 2. MAGEA3 Knockdown Contributes to Suppressed Proliferation and Invasion but Promoted Apoptosis of HepG2 Cells

(A) The mRNA level of MAGEA3 in HepG2 cells transfected with designated siRNAs determined by qRT-PCR. (B–D) The viability (B), apoptosis (C), and invasion (×200; D) of HepG2 cells upon transfection with si-MAGEA3 assessed by MTT, flow cytometry, and Transwell assays, respectively. (E) Protein expression of E-cadherin in HepG2 cells measured using western blot analysis. Measurement data were expressed as mean ± SD. Differences among groups at different points of time were assessed with repeated-measures ANOVA. The comparisons among multiple groups were assessed with one-way ANOVA, followed by Tukey's post hoc test. Each experiment was repeated three times. *$p < 0.05$ versus the mock- or si-NC-transfected cells.

depletion ($p < 0.05$) (Figure 3A). Multidrug resistance-associated protein 2 (MRP2), MRP3, and multidrug resistance protein 1 (MDR-1), the hepatobiliary transporters, induce chemoresistance of HCC cells and significantly limit the therapeutic efficiency of chemotherapy in HCC patients.[5,21] Moreover, as displayed in Figures 3B and 3C, the expression of MRP2, MRP3, and MDR-1 was reduced upon silence of MAGEA3. ELISA detection of albumin (ALB) in the supernatant of HepG2 cells showed that knocking down MAGEA3 elevated ALB content (Figure 3D). Further, consistent regulatory effects of si-MAGEA3 on HepG2 cells were detected in Huh7 cells (Figure S2). Thus, MAGEA3 knockdown might efficiently decrease the resistance of HepG2 cells and Huh7 cells to cisplatin.

miR-31-5p Targets MAGEA3 and Represses HCC Development *In Vitro* as well as Chemoresistance of HCC Cells to Cisplatin

As mentioned above, miR-31-5p and miR-448 were predicated to target MAGEA3, and further analysis in the TargetScan database revealed that miR-31-5p/miR-448 might target the 3′ UTR of MAGEA3 (Figure 4A).

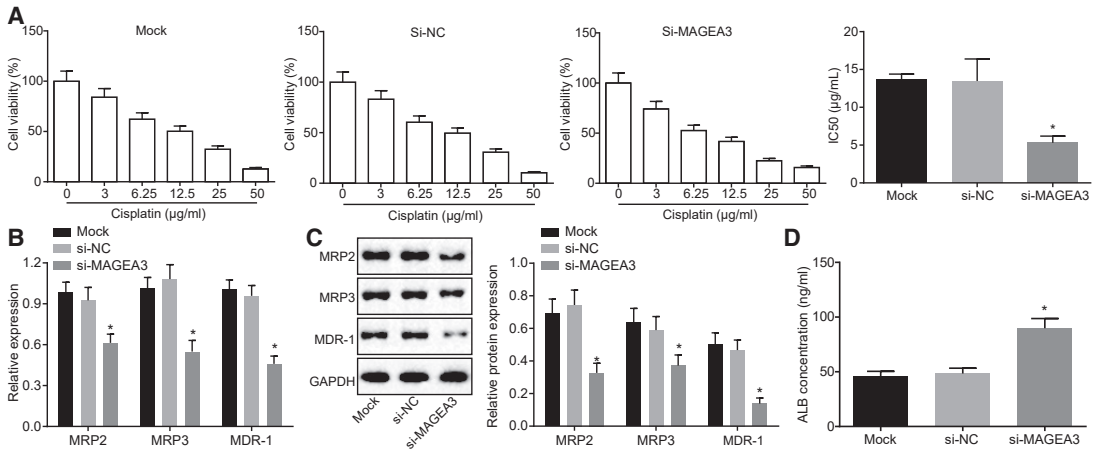

Figure 3. The Knockdown of MAGEA3 Reduces the Resistance of HepG2 Cells to Cisplatin

(A) CCK-8 assay showing viability and the IC_{50} of HepG2 cells transfected with mock, si-NC, or si-MAGEA3 upon treatment with cisplatin at different concentrations. (B) The mRNA levels of MRP2, MRP3, and MDR-1 in HepG2 cells transfected with si-MAGEA3 upon cisplatin treatment determined by qRT-PCR. (C) The protein levels of MRP2, MRP3, and MDR-1 in HepG2 cells transfected with si-MAGEA3 upon cisplatin treatment measured using western blot analysis. (D) ALB content in the supernatant of HepG2 cells in response to si-MAGEA3 transfection detected by ELISA. Measurement data were expressed as mean ± SD. The comparisons among multiple groups were assessed with one-way ANOVA, followed by Tukey's post hoc test. Each experiment was repeated three times. *$p < 0.05$ versus the mock- or si-NC-transfected cells.

As shown in Figure 4B, upon overexpression of miR-31-5p or miR-448, luciferase activity was significantly reduced in HepG2 cells transfected with pmirGLO vector containing the 3′ UTR of MAGEA3. Additionally, luciferase activity of HepG2 cells transfected with pmirGLO vector containing the mutated 3′ UTR of MAGEA3 was not influenced by miR-31-5p or miR-448 expression (Figure 4B), demonstrating the specificity of the binding of miR-31-5p and miR-448 to the 3′ UTR of MAGEA3. Therefore, both miR-31-5p and miR-448 could directly target MAGEA3.

Considering that miR-31-5p triggered more significant post-transcriptional downregulation of MAGEA3, miR-31-5p was applied for subsequent use in the present study. Initially, MTT assay was adopted to measure the influence of miR-31-5p on the viability of HepG2 cells and Huh7 cells, and the decreased growth rates upon miR-31-5p mimic transfection were observed (Figure 4C; Figure S3A). Additionally, enforced miR-31-5p expression contributed to suppressed invasion of HepG2 cells and Huh7 cells (Figure 4D; Figure S3B), downregulated protein expression of E-cadherin in HepG2 cells and Huh7 cells (Figure 4G; Figure S3E), and enhanced apoptosis of HepG2 cells and Huh7 cells (Figure 4E; Figure S3C). Furthermore, the effect of miR-31-5p on HCC cell chemoresistance to cisplatin was assessed, and it was found that miR-31-5p mimic transfection resulted in reduced IC_{50} in HepG2 cells and Huh7 cells (Figure 4F; Figure S3D), together with downregulated expression of MRP2, MRP3, MDR-1 (Figure 4G; Figure S3E), and elevated content of ALB (Figure 4H; Figure S3F). Collectively, miR-31-5p suppressed the progression of HCC *in vitro* and reduced HCC cell chemoresistance to cisplatin.

LINC01234 Silencing Represses MAGEA3-Dependent HCC Progression by Negatively Mediating miR-31-5p

RNA-fluorescence *in situ* hybridization (FISH) exhibited that LINC01234 was mainly located in the cytoplasm of HepG2 cells and Huh7 cells (Figure 5A; Figure S4A), suggesting that LINC01234 might exert regulatory function in the cytoplasm. As bioinformatics analysis showed that LINC01234 could bind to miR-31-5p, a dual-luciferase reporter gene assay was employed to analyze this relationship. As shown in Figure 5B and Figure S4B, luciferase activity of the pmirGLO vector containing the LINC01234 sequence was notably decreased upon miR-31-5p expression in HepG2 cells and Huh7 cells. However, luciferase activity of the pmirGLO vector containing the mutated LINC01234 sequence was hardly affected by miR-31-5p mimic transfection (Figure 5B; Figure S4B).

Furthermore, the data from the RNA pull-down assay exhibited that LINC01234 was abundantly enriched in the wild-type miR-31-5p group in comparison with the negative control (NC) or mutated miR-31-5p group ($p < 0.05$) (Figure 5C; Figure S4C). These data revealed the specific binding between LINC01234 and miR-31-5p. Meanwhile, RNA-binding protein immunoprecipitation (RIP) experiments were performed, and both HepG2 and Huh7 cell lysate were incubated with antibody to Argonaute 2 (Ago2) or DICER, the effector component of the RISC complex. As shown in Figure 5D and Figure S4D, enrichment of LINC01234 in Ago2- or DICER-immunoprecipitated complex was increased in comparison with the control immunoglobulin G (IgG)-immunoprecipitated complex ($p < 0.05$), indicating that LINC01234 could bind to Ago2 or DICER.

Expression of LINC01234 in HepG2 cells and Huh7 cells was silenced in order to explore the functions of LINC01234. As determined by qRT-PCR, knocking down LINC01234 reduced MAGEA3 expression in HepG2 cells and Huh7 cells; however, increase of MAGEA3 caused by si-LINC01234 was inhibited by miR-31-5p inhibitor (Figure 5E; Figure S4E). Besides, data of the RNA pull-down assay demonstrated that silencing of LINC01234 could enhance the binding of miR-31-5p

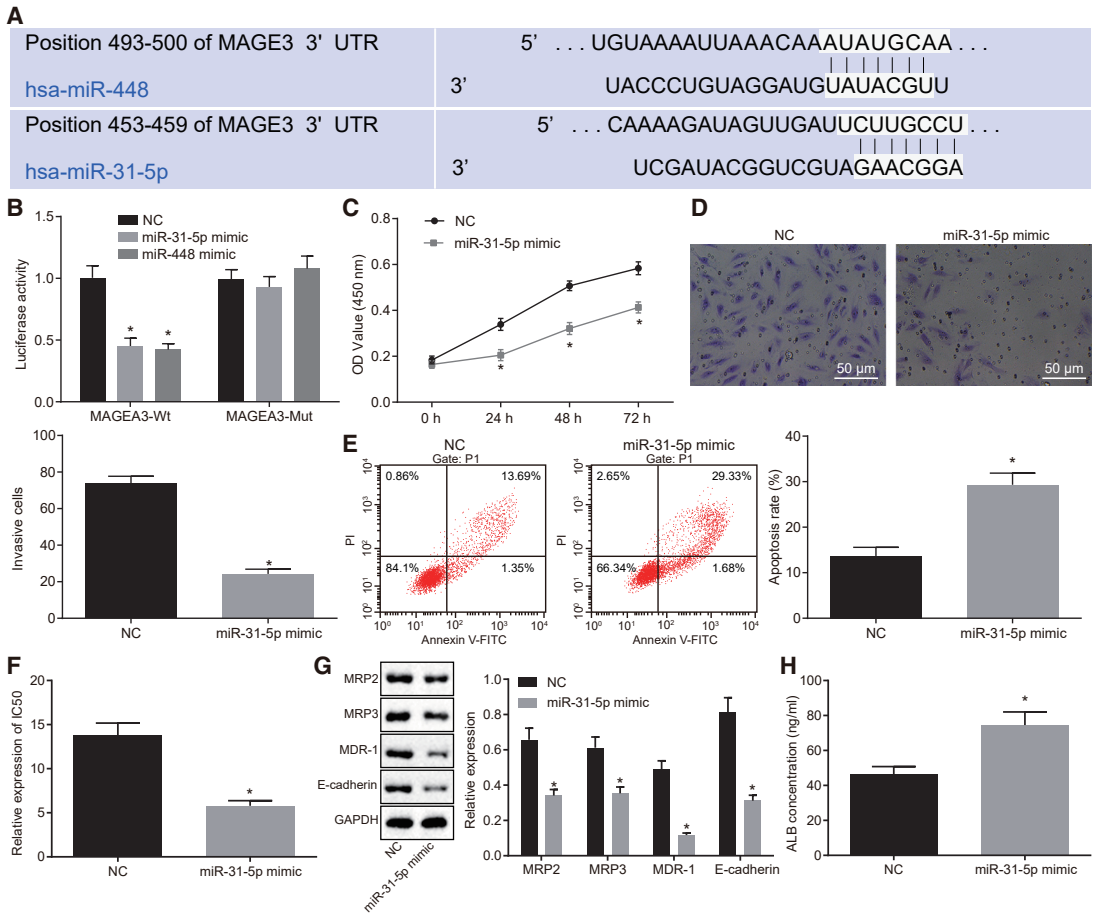

Figure 4. Upregulation miR-31-5p Hinders HCC Progression and Chemoresistance of HepG2 Cells to Cisplatin by Depleting MAGEA3

(A) The binding sites of miR-31-5p and miR-448 in the 3′ UTR region of MAGEA3 predicted by TargetScan. (B) The luciferase activity of MAGEA3-WT and MAGEA3-Mut in HepG2 cells after miR-31-5p or miR-448 mimic transfection. (C–E) The viability (C), invasion (×200; D), and cisplatin-induced apoptosis (E) of HepG2 cells following miR-31-5p mimic transfection evaluated by MTT assay, Transwell assay, and flow cytometry, respectively. (F) IC_{50} value of HepG2 cells following miR-31-5p mimic transfection. (G) Western blot analysis showing protein expression of MRP2, MRP3, MDR-1, and E-cadherin in HepG2 cells after restoration of miR-31-5p. (H) Content of ALB in supernatant of HepG2 cells following overexpression of miR-31-5p detected by ELISA. Measurement data were expressed as mean ± SD. The comparison between the two groups was analyzed by independent sample t test and the comparisons among multiple groups by one-way ANOVA, followed by Tukey's post hoc test. Each experiment was repeated three times. *$p < 0.05$ versus the NC-transfected cells.

to MAGEA3 (Figure 5F; Figure S4F). Moreover, depletion of LINC01234 suppressed viability (Figure 5G; Figure S4G) and invasion (Figure 5H; Figure S4H) and downregulated the protein expression of E-cadherin (Figure 5K; Figure S4K), but it promoted cisplatin-induced apoptosis (Figure 5I; Figure S4I) of HepG2 cells and Huh7 cells. Additionally, it was found that when compared with si-NC transfection, si-LINC01234 transfection led to a reduced IC_{50} value in HepG2 cells and Huh7 cells (Figure 5J; Figure S4J), downregulated protein expression of MRP2, MRP3, and MDR-1 (Figure 5K; Figure S4K), but upregulated expression of ALB (Figure 5L; Figure S4L). However, the anti-proliferative, pro-apoptotic, and chemosensitizing effects of LINC01234 silencing were reversed through miR-31-5p depletion. Collectively, reduction of LINC01234 upregulated miR-31-5p to downregulate MAGEA3 expression, thereby further suppressing malignant phenotype of HCC cells.

DISCUSSION

Currently, HCC prognosis in patients at late stage remains poor.[22] In the current study, LINC01234 and MAGEA3 were found to be upregulated in HCC in accordance to TCGA data and could bind to miR-31-5p. Since the interactions among the three factors remain to be clarified, our study was conducted to elucidate the mechanism of how they function in the progression and chemoresistance of HCC.

The dysregulated expression of lncRNAs is associated with HCC tumors.[23] HCC-related lncRNAs can mediate cell proliferation, apoptosis, invasion, metastasis, as well as angiogenesis, thereby participating in diverse processes during HCC progression.[24] Several lncRNAs are evident to have a high expression in HCC, such as uc003wbd, AF085935, and BANCR.[25,26] LINC01234 is upregulated in stomach adenocarcinoma,[27] but its role remains

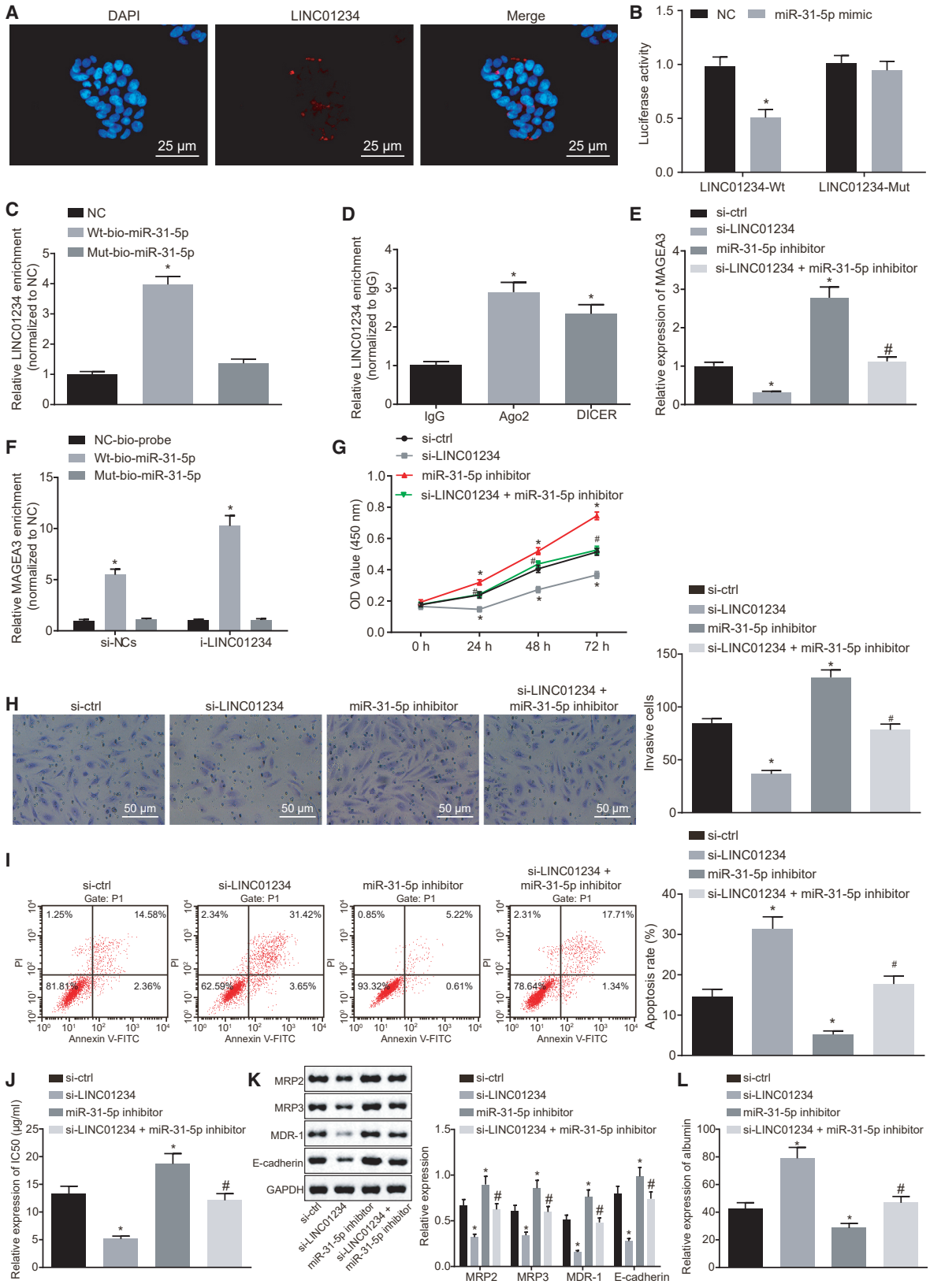

(legend on next page)

unknown in HCC. The findings from the study displayed that siRNA-mediated silencing of LINC01234 could suppress proliferation and invasion of both HepG2 and Huh7 cells while elevating cisplatin-induced cell apoptosis. Hence, our data suggest that downregulation of LINC01234 could exert an inhibitory effect on HCC progression and a chemosensitizing effect. This might provide insightful therapeutic targets for HCC. Recently, multiple studies have revealed that lncRNAs could interact with miRNAs to function in diseases and human cancers.[28,29] Our results revealed that LINC01234 regulated miR-31-5p to mediate HCC progression. Silencing of LINC01234 upregulated miR-31-5p to restrain malignant phenotypes of HCC cells and to enhance cisplatin-induced apoptosis.

miR-31-5p has been revealed to be poorly expressed in prostate cancer.[30] A recent study has identified a close relationship between miR-31-5p and liver function.[31] Also, a large number of miRNAs negatively target genes by binding to 3′ UTR regions.[32] Furthermore, it was confirmed that MAGEA3 was a target of miR-31-5p, which is in line with previous studies conducted.[33,34] Additionally, the current study further demonstrates that MAGEA3 silencing reduced HepG2 and Huh7 cell proliferation and invasion, while also increasing cell apoptosis *in vitro*. In this study, RNA pull-down and RIP assays identified the binding between LINC01234 and MAGEA3 to miR-31-5p. It is speculated that LINC01234 reduction could upregulate miR-31-5p to inhibit MAGEA3, leading to suppression in malignant phenotype of HCC cells.

MRPs are ATP-binding cassette transporters, endowing tumor cells with multidrug resistance via reducing the uptake of anticancer drugs.[35] Downregulation of MDR-1 and MRP could lead to intracellular accumulation of anticancer drugs to enhance the efficiency of chemotherapy.[36] Besides, MDR-1 gene polymorphism (c.4125A > C) is associated with HCC susceptibility in the Chinese population and may be a risk factor.[37,38] Thus, the MDR-1 gene may be a potential target for HCC treatment. It was also found that MAGEA3 depletion diminished the resistance of HepG2 cells to cisplatin by reducing MRP2, MRP3, and MDR-1. The results obtained from the study are consistent with a previous report that miRNA double-strand fragments mediated knockdown of MAGEA3 leads to the reduced cell proliferation and enhanced docetaxel sensitivity in gastric cancer-derived cells.[39] Recently, the correlation between lncRNAs and chemoresistance in HCC has also been identified.[40,41] According to aforementioned results, silencing of LINC01234 could overcome HCC cell chemoresistance through MAGEA3 depletion.

In conclusion, LINC01234 downregulation could suppress the progression and chemoresistance in HCC by reducing miR-31-5p-mediated inhibition of MAGEA3 (Figure 6). Importantly, MAGEA3 could confer cisplatin resistance to HCC cells, and the LINC01234/miR-31-5p regulatory network might participate in the process. However, whether the LINC01234/miR-31-5p/MAGEA3 axis is involved in the modulation of HCC chemoresistance to other anticancer drugs needs to be further investigated. Besides, *in vivo* experiments should be conducted to further elucidate the mechanisms and verify whether the pathway plays a critical role in animals.

MATERIALS AND METHODS

Bioinformatics Prediction

To identify HCC-related genes, microarray data of HCC were acquired from TCGA database (http://cancergenome.nih.gov/about-nci/organization/ccg/research/structural-genomics/tcga), followed by differential analysis with the edgeR package.[42] The FDR of genes was obtained by p value correction using package multitest. Then, DEGs were screened out with the threshold of FDR <0.05 and |log2 (fold change)| > 2.

Cell Culture

HepG2 cells (American Type Culture Collection, Manassas, VA, USA) and Huh7 cells (Shanghai Institutes for Biological Sciences, Chinese Academy of Sciences, Shanghai, China) (http://www.cellbank.org.cn/index.asp) were cultured in DMEM containing 10% fetal bovine serum (FBS) in a 5% CO_2 incubator at 37°C. The adhered cells were passaged and detached by applying 0.25% trypsin (Hyclone, Logan, UT, USA). Cells in logarithmic growth period were used for further experiments.

Transient Transfection

Both HepG2 and Huh7 cells were seeded into 50-mL culture bottles and grown in complete medium to reach 50%–60% confluence. A total of 5 μL Lipofectamine 2000 transfection reagents, 100 μL serum-free medium, and 50 nmol RNA was mixed in accordance to the guidelines provided by the Lipofectamine 2000 transfection kit (11668019, Invitrogen, Carlsbad, CA, USA) and added into the cells after incubation. After 6–8 h of transfection, the medium was replaced with fresh complete medium. Transfected RNAs, including

Figure 5. Depleted LINC01234 Enhances miR-31-5p-Mediated Downregulation of MAGEA3 to Prevent HCC Progression

(A) The subcellular localization of LINC01234 in HepG2 cells identified by FISH (×400). (B) The luciferase activity of LINC01234 in HepG2 cells upon miR-31-5p mimic transfection in a dual-luciferase reporter system. (C) The binding between LINC01234 and miR-31-5p detected by RNA pull-down. (D) The binding between LINC01234 and Ago2 or DICER detected by RIP. (E) MAGEA3 expression in HepG2 cells in response to altered expression of LINC01234 and/or miR-31-5p measured using qRT-PCR. (F) Binding of miR-31-5p to MAGEA3 in HepG2 cells detected using RNA pull-down. (G–I) The viability (G), invasion (×200; H), and cisplatin-induced apoptosis (I) of HepG2 cells upon inhibition of LINC01234 and/or miR-31-5p assessed using MTT, Transwell, and flow cytometry assays. (J) IC_{50} value of HepG2 cells upon inhibition of LINC01234 and/or miR-31-5p. (K) Protein expression of MRP2, MRP3, MDR-1, and E-cadherin in HepG2 cells upon inhibition of LINC01234 and/or miR-31-5p determined using western blot analysis. (L) ALB content in the supernatant of HepG2 cells upon inhibition of LINC01234 and/or miR-31-5p detected by ELISA. Measurement data were expressed as mean ± SD. Differences among groups at different points of time were assessed with repeated-measures ANOVA. The comparison between two groups was analyzed by independent sample t test and the comparisons among multiple groups by one-way ANOVA, followed by Tukey's post hoc test. Each experiment was repeated three times. *p < 0.05 versus the IgG immunoprecipitates or the NC- or si-ctrl-transfected cells; #p < 0.05 versus the si-LINC01234-transfected cells.

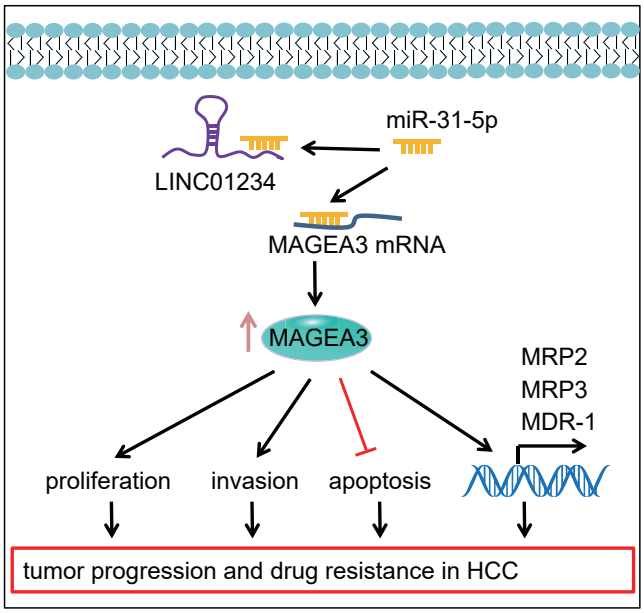

Figure 6. The LINC01234/miR-31-5p/MAGEA3 Axis Is Involved in Modulation of HCC Progression and Cisplatin Resistance

Downregulated LINC01234 increases miR-31-5p expression, thus reducing MAGEA3 expression in HCC cells. Subsequently, the proliferation and invasion of HCC cells were attenuated, while the apoptosis was enhanced. In addition, the reduced expression of MRP2, MRP3, and MDR-1 were detected during these processes.

mimic, inhibitor, siRNA were all synthesized by GenePharma (Shanghai, China).

RNA Extraction and Quantification

Total RNA extracted from HepG2 cells and Huh7 cells was reversely transcribed into cDNA with a reverse transcription kit (Beijing TransGen Biotech, Beijing, China). qPCR was performed by applying the SYBR Premix Ex Taq II kit (TaKaRa Biotechnology (Dalian), Liaoning, China) on an ABI7500 instrument (Applied Biosystems, Carlsbad, CA, USA). The primers (Table 1) were synthesized by Shanghai Sangon Biotechnology (Shanghai, China). Glyceraldehyde-3-phosphate dehydrogenase (GAPDH) and U6 were used as internal references, and the fold changes were calculated by means of relative quantification ($2^{-\Delta\Delta Ct}$ method).[43]

MTT Assay for Cell Viability

At the time points of 0, 24, 48, and 72 h post-transfection, both HepG2 and Huh7 cells were incubated with MTT. After incubation, dimethyl sulfoxide was added to dissolve the produced formazan. The optical density value was measured at 570 nm using an enzyme immunoassay analyzer (ZY057877, Beijing Zhongyi Kexin Technology, Beijing, China). Mean values were calculated from cell samples in three replicate wells.

Transwell Assay for Cell Invasion

Transwell assay was conducted 24 h post-transfection. After being detached and suspended in serum-free DMEM medium, HepG2 cells and Huh7 cells were starved in serum-free culture medium for 24 consecutive h. After detachment, the cells were dispersed to cell suspension at a density of 3×10^5 cells/mL. Then, 100 μL HepG2 cell suspension or 100 μL Huh7 cell suspension was added into the apical chamber pre-coated with Matrigel (1:10, Becton Dickinson, Franklin Lakes, NJ, USA), while 600 μL DMEM medium containing 10% serum (as the chemokine) was added to the basolateral chamber. In accordance with the manufacturer's protocols of Transwell system (Corning, Corning, NY, USA), the total number of transmembrane cells was tallied via crystal violet staining.

Flow Cytometry for Cell Apoptosis

An Annexin V-fluorescein isothiocyanate/propidium iodide (Annexin V-FITC/PI) detection kit (556547, Shanghai Shuojia Biotechnology, Shanghai, China) was utilized to measure apoptosis of HepG2 cells and Huh7 cells. After 48 h of transfection, HepG2 cells and Huh7 cells were further treated with cisplatin (3 μg/mL) for 48 h. In brief, cells were centrifuged at 2,000 rpm for 5 min, suspended in pre-cold 1× PBS, and then centrifuged again at 200 rpm for 5–10 min. Next, cells were resuspended in 300 μL 1× binding buffer, and 5 μL Annexin V-FITC was added, followed by 15 min of incubation in avoidance of light. Then, 5 μL PI solution was added and incubated in ice bath under dark conditions for 5 min. Fluorescence intensities were determined using the Partec Cube 6 flow cytometer (Partec, Munster, Germany) using the excitation wavelength at 480 nm and a 530-nm band-pass filter for FITC detection and a 575-nm long-pass filter for PI detection. Annexin V-FITC-stained cells presented green fluorescence, and non-vital PI-stained cells were displayed in a red fluorescence. Based on the staining fluorescence, intact cells ($FITC^-PI^-$), apoptotic cells at early stage ($FITC^+PI^-$), and apoptotic cells at late stage or necrotic cells ($FITC^+PI^+$) were discriminated.

CCK-8 Assay for Drug Resistance

After 48 consecutive h of transfection, HepG2 cells and Huh7 cells were collected and seeded into a 96-well plate (1×10^4 cells/well). The adhered cells were then cultured in a series of medium with an increasing dose of cisplatin (0, 2.5, 5, 10, 20, and 40 μg/mL) for 48 h. Next, the cells were incubated with 10% CCK-8 solution (JK-021, Shanghai Jingke Chemical Technology, Shanghai, China) in the dark for 2 h. The absorbance at 450 nm was detected using a microplate reader, and the IC_{50} of cisplatin was calculated.

Western Blot Analysis

Total proteins were extracted from HepG2 cells and Huh7 cells using radio-immunoprecipitation assay lysis buffer (Beyotime Biotechnology, Shanghai, China). After protein quantitation using the bicinchoninic acid assay, the proteins were separated by PAGE with a 5% stacking gel and a 10% separating gel and then transferred onto a nitrocellulose membrane using wet transfer apparatus. Next, the membrane was blocked with 5% BSA for 1 h and incubated with the diluted rabbit anti-human antibodies from Abcam (Cambridge, UK) at 4°C overnight: MDR-1 (ab129450, 1:1,000), MRP2 (ab203397, 1:500), MRP3 (ab107083, 1:250), GAPDH (ab37168,

Table 1. Primer Sequences for qRT-PCR

Gene	Sequence
LINC01234	F, 5′-TCACCTCCTCGGTCTCAGTT-3′
	R, 5′-GGGTGAGAAGAGACAAGCGT-3′
miR-31-5p	F, 5′-GTCGTATCCAGTGCAGGGTCCGA GGTATTCGCACTGGATACGACAGCTAT-3′
	R, 5′-TAATACTGCCTGGTAATGATGA-3′
MAGEA3	F, 5′-GAAGCCGCCCCAGGCTCG-3′
	R, 5′-GGAGTCCTCATAGGATTGGCTCC-3′
MRP2	F, 5′-CCTCACAAACTGCCTCTTCA-3′
	R, 5′-AGCCCAATGGAAGCAATATC-3′
MRP3	F, 5′-ACAACCTCATCCAGGCTACC-3′
	R, 5′-GGTTGGCTGGAGAATCAAAT-3′
MDR-1	F, 5′-ATGCCTTCATCGAGTCACTG-3′
	R, 5′-TAACAAGGGCACGAGCTATG-3′
U6	F, 5′-GTCGTATCCAGTGCAGGGTCCGAGG TGCACTGGATACGACAAAATATGGAAC-3′
	R, 5′-GTGCTCGCTTCGGCAGC-3′
GAPDH	F, 5′-CGGAGTCAACGGATTTGGTCGTAT-3′
	R, 5′-AGCCTTCTCCATGGTGGTGAAGAC-3′

miR-31-5p, microRNA-31-5p; MAGEA3, melanoma-associated antigen A3; MRP2, multidrug resistance-associated protein 2; MDR-1, multidrug resistance protein 1; GAPDH, glyceraldehyde-3-phosphate dehydrogenase; F, forward; R, reverse.

1 μg/mL), and E-cadherin (ab15148, 1:500). Next, the membrane was washed using PBS/Tween-20 and further incubated by applying 5% skimmed milk-diluted secondary antibody goat anti-rabbit IgG (ab205718, 1: 5000) for 1 h in avoidance of light. Subsequently, the protein bands were developed and visualized in a gel imaging system (MG8600, Bio-Rad, Hercules, CA, USA). Images were analyzed using the Image-Pro Plus software (Version 7.0, Media Cybernetics, Silver Springs, MD, USA). The expression levels of target proteins relative to GAPDH were calculated.

ELISA

According to the protocols of the ELISA kits (R&D Systems, Minneapolis, MN, USA), the content of ALB in cell supernatant was measured.

RNA-FISH

The subcellular localization of LINC01234 in HepG2 cells and Huh7 cells was detected in strict accordance to the guidelines provided by the FISH kit (C10910, RiboBio, Guangzhou, Guangdong, China). The cells were detached and cultured in the 24-well plate. Upon reaching 60%–70% confluence, cells were rinsed using 1× PBS, followed by 4% paraformaldehyde fixation. Next, cells were permeabilized for 5 min at 4°C and blocked in 200 μL pre-hybridization solution at 37°C for 30 min. Meanwhile, the hybridization solution was pre-heated and mixed with 2.5 μL 20 μM FISH probe mix. Cells were incubated with 1 mL probe-containing hybridization solution at 37°C overnight in avoidance of light. After the cells were washed, they were stained using DAPI for 10 min and sealed prior to fluorescence detection. The probes against LINC01234 were synthesized by RiboBio (Guangzhou, Guangdong, China).

Dual-Luciferase Reporter Assay

The sequence of LINC01234 and the 3′ UTR of MAGEA3 were cloned into the pmirGLO vectors (E1330, Promega, Madison, WI, USA) to generate LINC01234-wild-type (WT) and MAGEA3-WT plasmids. Next, site-specific mutagenesis was performed to create LINC01234 mutant (Mut) and MAGEA3-Mut plasmids. The pRL-TK renilla luciferase reporter vector (E2241, Promega, Madison, WI, USA) was used as the internal reference. Both NC and miR-31-5p mimic were co-transfected with the constructed luciferase reporter vectors into HepG2 cells or Huh7 cells. The relative luciferase activity was calculated as the ratio of the signal of firefly luciferase to that of renilla luciferase. The luciferase signals were measured in strict accordance to the guidelines provided by the dual-luciferase reporter gene assay kit (GM-040502A, Qcbio Science and Technologies, Shanghai, China) at 560 nm for the firefly luciferase and 465 nm for the renilla luciferase.

RNA Pull-Down

In brief, HepG2 cells and Huh7 cells were treated using 50 nM biotinylated WT miR-31-5p (WT-bio-miR-31-5p) or Mut miR-31-5p (Mut-bio-miR-31-5p). After 48 consecutive h, the cells were collected and lysed with specific lysis buffer (Ambion, Austin, TX, USA) for 10 min. The lysate was then incubated with M-280 streptavidin magnetic beads (S3762, Sigma-Aldrich, St. Louis, MO, USA) pre-coated using RNase-free BSA and yeast tRNA (TRNABAK-RO, Sigma-Aldrich, St. Louis, MO, USA) at 4°C for 3 h. The beads were then washed using the following buffer: pre-cold lysis buffer (two times), low-salt buffer (three times), and high-salt buffer. After the bound RNA was purified using the Trizol reagent, qRT-PCR was performed to analyze LINC01234 content.

RIP

HepG2 cells and Huh7 cells were lysed using the lysis buffer (25 mM Tris-HCl [pH 7.4], 150 mM NaCl, 0.5% Nonidet P-40, 2 mM ethylene diamine tetraacetic acid, 1 mM NaF, and 0.5 mM dithiothreitol) containing RNasin (Takara Bio, Otsu, Shiga, Japan) and protease inhibitor (B14001a, Roche, Madison, WI, USA). The lysate was then centrifuged for 30 min, and the supernatant was subjected to immunoprecipitation with anti-Ago2 or anti-DICER antibody-coated magnetic beads (BMFA-1, Biomarker Technologies, Beijing, China) or anti-IgG-coated magnetic beads as the control. After incubation at 4°C for 4 h, the beads were washed three times using the wash buffer (50 mM Tris-HCl, 300 mM NaCl [pH 7.4], 1 mM $MgCl_2$, 0.1% Nonidet P-40). Finally, RNA was extracted with Trizol reagent from the beads, followed by qRT-PCR detection.

Statistical Analysis

All experimental data were processed and analyzed using SPSS 22.0 statistical software (IBM, Armonk, NY, USA). The data are presented

as mean ± SD. The differences between two groups were compared using an independent sample t test. Comparisons among multiple groups were analyzed using one-way ANOVA, followed by Tukey's post hoc test. Statistical significance was considered at $p < 0.05$.

SUPPLEMENTAL INFORMATION

Supplemental Information can be found online at https://doi.org/10.1016/j.omtn.2019.10.035.

AUTHOR CONTRIBUTIONS

Y.C. and H.Z. designed the study. C.Q., H.L., and X.F. collated the data. H.T., J.Z., and B.F. carried out data analyses and produced the initial draft of the manuscript. Y.C., H.Z., and C.Q. contributed to drafting the manuscript. All authors have read and approved the final submitted manuscript.

CONFLICT OF INTEREST

The authors declare no competing interests.

ACKNOWLEDGMENTS

We acknowledge and appreciate our colleagues for their valuable efforts and comments on this paper.

REFERENCES

1. Global Burden of Disease Cancer Collaboration, Fitzmaurice, C., Allen, C., Barber, R.M., Barregard, L., Bhutta, Z.A., Brenner, H., Dicker, D.J., Chimed-Orchir, O., Dandona, R., Dandona, L., et al. (2017). Global, Regional, and National Cancer Incidence, Mortality, Years of Life Lost, Years Lived With Disability, and Disability-Adjusted Life-years for 32 Cancer Groups, 1990 to 2015: A Systematic Analysis for the Global Burden of Disease Study. JAMA Oncol. *3*, 524–548.
2. McGlynn, K.A., Petrick, J.L., and London, W.T. (2015). Global epidemiology of hepatocellular carcinoma: an emphasis on demographic and regional variability. Clin. Liver Dis. *19*, 223–238.
3. Lafaro, K.J., Demirjian, A.N., and Pawlik, T.M. (2015). Epidemiology of hepatocellular carcinoma. Surg. Oncol. Clin. N. Am. *24*, 1–17.
4. Osaki, A., Suda, T., Kamimura, K., Tsuchiya, A., Tamura, Y., Takamura, M., Igarashi, M., Kawai, H., Yamagiwa, S., and Aoyagi, Y. (2013). A safe and effective dose of cisplatin in hepatic arterial infusion chemotherapy for hepatocellular carcinoma. Cancer Med. *2*, 86–98.
5. Lohitesh, K., Chowdhury, R., and Mukherjee, S. (2018). Resistance a major hindrance to chemotherapy in hepatocellular carcinoma: an insight. Cancer Cell Int. *18*, 44.
6. Dhir, M., Melin, A.A., Douaiher, J., Lin, C., Zhen, W.K., Hussain, S.M., Geschwind, J.F., Doyle, M.B., Abou-Alfa, G.K., and Are, C. (2016). A Review and Update of Treatment Options and Controversies in the Management of Hepatocellular Carcinoma. Ann. Surg. *263*, 1112–1125.
7. Bruix, J., Reig, M., and Sherman, M. (2016). Evidence-Based Diagnosis, Staging, and Treatment of Patients With Hepatocellular Carcinoma. Gastroenterology *150*, 835–853.
8. Sun, Z., Zhu, Y., Xia, J., Sawakami, T., Kokudo, N., and Zhang, N. (2016). Status of and prospects for cancer vaccines against hepatocellular carcinoma in clinical trials. Biosci. Trends *10*, 85–91.
9. Lian, Y., Sang, M., Gu, L., Liu, F., Yin, D., Liu, S., Huang, W., Wu, Y., and Shan, B. (2017). MAGE-A family is involved in gastric cancer progression and indicates poor prognosis of gastric cancer patients. Pathol. Res. Pract. *213*, 943–948.
10. Sang, M., Gu, L., Yin, D., Liu, F., Lian, Y., Zhang, X., Liu, S., Huang, W., Wu, Y., and Shan, B. (2017). MAGE-A family expression is correlated with poor survival of patients with lung adenocarcinoma: a retrospective clinical study based on tissue microarray. J. Clin. Pathol. *70*, 533–540.
11. Esfandiary, A., and Ghafouri-Fard, S. (2015). MAGE-A3: an immunogenic target used in clinical practice. Immunotherapy *7*, 683–704.
12. Chen, X., Wang, L., Liu, J., Huang, L., Yang, L., Gao, Q., Shi, X., Li, J., Li, F., Zhang, Z., et al. (2017). Expression and prognostic relevance of MAGE-A3 and MAGE-C2 in non-small cell lung cancer. Oncol. Lett. *13*, 1609–1618.
13. Ayers, D., and Vandesompele, J. (2017). Influence of microRNAs and Long Non-Coding RNAs in Cancer Chemoresistance. Genes (Basel) *8*, E95.
14. Zhao, G., Han, C., Zhang, Z., Wang, L., and Xu, J. (2017). Increased expression of microRNA-31-5p inhibits cell proliferation, migration, and invasion via regulating Sp1 transcription factor in HepG2 hepatocellular carcinoma cell line. Biochem. Biophys. Res. Commun. *490*, 371–377.
15. Li, M., Chen, W., Zhang, H., Zhang, Y., Ke, F., Wu, X., Zhang, Y., Weng, M., Liu, Y., and Gong, W. (2016). MiR-31 regulates the cisplatin resistance by targeting Src in gallbladder cancer. Oncotarget *7*, 83060–83070.
16. Cesana, M., Cacchiarelli, D., Legnini, I., Santini, T., Sthandier, O., Chinappi, M., Tramontano, A., and Bozzoni, I. (2011). A long noncoding RNA controls muscle differentiation by functioning as a competing endogenous RNA. Cell *147*, 358–369.
17. Yang, S., Ning, Q., Zhang, G., Sun, H., Wang, Z., and Li, Y. (2016). Construction of differential mRNA-lncRNA crosstalk networks based on ceRNA hypothesis uncover key roles of lncRNAs implicated in esophageal squamous cell carcinoma. Oncotarget *7*, 85728–85740.
18. Huang, X., Gao, Y., Qin, J., and Lu, S. (2018). lncRNA MIAT promotes proliferation and invasion of HCC cells via sponging miR-214. Am. J. Physiol. Gastrointest. Liver Physiol. *314*, G559–G565.
19. Guo, L., Peng, Y., Meng, Y., Liu, Y., Yang, S., Jin, H., and Li, Q. (2017). Expression profiles analysis reveals an integrated miRNA-lncRNA signature to predict survival in ovarian cancer patients with wild-type BRCA1/2. Oncotarget *8*, 68483–68492.
20. Zhang, Y., Guan, D.X., Shi, J., Gao, H., Li, J.J., Zhao, J.S., Qiu, L., Liu, J., Li, N., Guo, W.X., et al. (2013). All-trans retinoic acid potentiates the chemotherapeutic effect of cisplatin by inducing differentiation of tumor initiating cells in liver cancer. J. Hepatol. *59*, 1255–1263.
21. Zollner, G., Wagner, M., Fickert, P., Silbert, D., Fuchsbichler, A., Zatloukal, K., Denk, H., and Trauner, M. (2005). Hepatobiliary transporter expression in human hepatocellular carcinoma. Liver Int. *25*, 367–379.
22. Giannini, E.G., Farinati, F., Ciccarese, F., Pecorelli, A., Rapaccini, G.L., Di Marco, M., Benvegnù, L., Caturelli, E., Zoli, M., Borzio, F., et al.; Italian Liver Cancer (ITA.LI.CA) group (2015). Prognosis of untreated hepatocellular carcinoma. Hepatology *61*, 184–190.
23. Zeisel, M.B., and Baumert, T.F. (2016). Translation and protein expression of lncRNAs: Impact for liver disease and hepatocellular carcinoma. Hepatology *64*, 671–674.
24. Huang, J.L., Zheng, L., Hu, Y.W., and Wang, Q. (2014). Characteristics of long non-coding RNA and its relation to hepatocellular carcinoma. Carcinogenesis *35*, 507–514.
25. Lu, J., Xie, F., Geng, L., Shen, W., Sui, C., and Yang, J. (2015). Investigation of serum lncRNA-uc003wbd and lncRNA-AF085935 expression profile in patients with hepatocellular carcinoma and HBV. Tumour Biol. *36*, 3231–3236.
26. Zhou, T., and Gao, Y. (2016). Increased expression of LncRNA BANCR and its prognostic significance in human hepatocellular carcinoma. World J. Surg. Oncol. *14*, 8.
27. Gu, J., Li, Y., Fan, L., Zhao, Q., Tan, B., Hua, K., and Wu, G. (2017). Identification of aberrantly expressed long non-coding RNAs in stomach adenocarcinoma. Oncotarget *8*, 49201–49216.
28. Guil, S., and Esteller, M. (2015). RNA-RNA interactions in gene regulation: the coding and noncoding players. Trends Biochem. Sci. *40*, 248–256.
29. Karreth, F.A., and Pandolfi, P.P. (2013). ceRNA cross-talk in cancer: when ce-bling rivalries go awry. Cancer Discov. *3*, 1113–1121.
30. Tsuchiyama, K., Ito, H., Taga, M., Naganuma, S., Oshinoya, Y., Nagano, K., Yokoyama, O., and Itoh, H. (2013). Expression of microRNAs associated with Gleason grading system in prostate cancer: miR-182-5p is a useful marker for high grade prostate cancer. Prostate *73*, 827–834.
31. Capri, M., Olivieri, F., Lanzarini, C., Remondini, D., Borelli, V., Lazzarini, R., Graciotti, L., Albertini, M.C., Bellavista, E., Santoro, A., et al. (2017). Identification

of miR-31-5p, miR-141-3p, miR-200c-3p, and GLT1 as human liver aging markers sensitive to donor-recipient age-mismatch in transplants. Aging Cell *16*, 262–272.

32. Zhou, P., Xu, W., Peng, X., Luo, Z., Xing, Q., Chen, X., Hou, C., Liang, W., Zhou, J., Wu, X., et al. (2013). Large-scale screens of miRNA-mRNA interactions unveiled that the 3'UTR of a gene is targeted by multiple miRNAs. PLoS ONE *8*, e68204.
33. Cui, Z., Yu, X., Guo, L., Wei, Y., Zheng, S., Li, W., Chen, P., Zhu, J., and Peng, J. (2013). Combined analysis of serum alpha-fetoprotein and MAGE-A3-specific cytotoxic T lymphocytes in peripheral blood for diagnosis of hepatocellular carcinoma. Dis. Markers *35*, 915–923.
34. Wang, C.Y., Lin, B.L., and Chen, C.H. (2016). An aptamer targeting shared tumor-specific peptide antigen of MAGE-A3 in multiple cancers. Int. J. Cancer *138*, 918–926.
35. Sodani, K., Patel, A., Kathawala, R.J., and Chen, Z.S. (2012). Multidrug resistance associated proteins in multidrug resistance. Chin. J. Cancer *31*, 58–72.
36. Xu, H.W., Xu, L., Hao, J.H., Qin, C.Y., and Liu, H. (2010). Expression of P-glycoprotein and multidrug resistance-associated protein is associated with multidrug resistance in gastric cancer. J. Int. Med. Res. *38*, 34–42.
37. Wang, Z.C., Liu, L.Z., Liu, X.Y., Hu, J.J., Wu, Y.N., Shi, J.Y., Yang, L.X., Duan, M., Wang, X.Y., Zhou, J., et al. (2015). Genetic polymorphisms of the multidrug resistance 1 gene MDR1 and the risk of hepatocellular carcinoma. Tumour Biol. *36*, 7007–7015.
38. Ren, Y.Q., Han, J.Q., Cao, J.B., Li, S.X., and Fan, G.R. (2012). Association of MDR1 gene polymorphisms with susceptibility to hepatocellular carcinoma in the Chinese population. Asian Pac. J. Cancer Prev. *13*, 5451–5454.
39. Xie, C., Subhash, V.V., Datta, A., Liem, N., Tan, S.H., Yeo, M.S., Tan, W.L., Koh, V., Yan, F.L., Wong, F.Y., et al. (2016). Melanoma associated antigen (MAGE)-A3 promotes cell proliferation and chemotherapeutic drug resistance in gastric cancer. Cell Oncol. (Dordr.) *39*, 175–186.
40. Jiang, M., Huang, O., Xie, Z., Wu, S., Zhang, X., Shen, A., Liu, H., Chen, X., Wu, J., Lou, Y., et al. (2014). A novel long non-coding RNA-ARA: adriamycin resistance-associated. Biochem. Pharmacol. *87*, 254–283.
41. Huo, X., Han, S., Wu, G., Latchoumanin, O., Zhou, G., Hebbard, L., George, J., and Qiao, L. (2017). Dysregulated long noncoding RNAs (lncRNAs) in hepatocellular carcinoma: implications for tumorigenesis, disease progression, and liver cancer stem cells. Mol. Cancer *16*, 165.
42. Robinson, M.D., McCarthy, D.J., and Smyth, G.K. (2010). edgeR: a Bioconductor package for differential expression analysis of digital gene expression data. Bioinformatics *26*, 139–140.
43. Xu, J., Lu, M.X., Cui, Y.D., and Du, Y.Z. (2017). Selection and Evaluation of Reference Genes for Expression Analysis Using qRT-PCR in Chilo suppressalis (Lepidoptera: Pyralidae). J. Econ. Entomol. *110*, 683–691.

OMTN, Volume *19*

Supplemental Information

LINC01234/MicroRNA-31-5p/MAGEA3 Axis Mediates the Proliferation and Chemoresistance of Hepatocellular Carcinoma Cells

Yunhao Chen, Hui Zhao, Haibo Li, Xiao Feng, Hui Tang, Jianwen Zhang, Binsheng Fu, and Chunhui Qiu

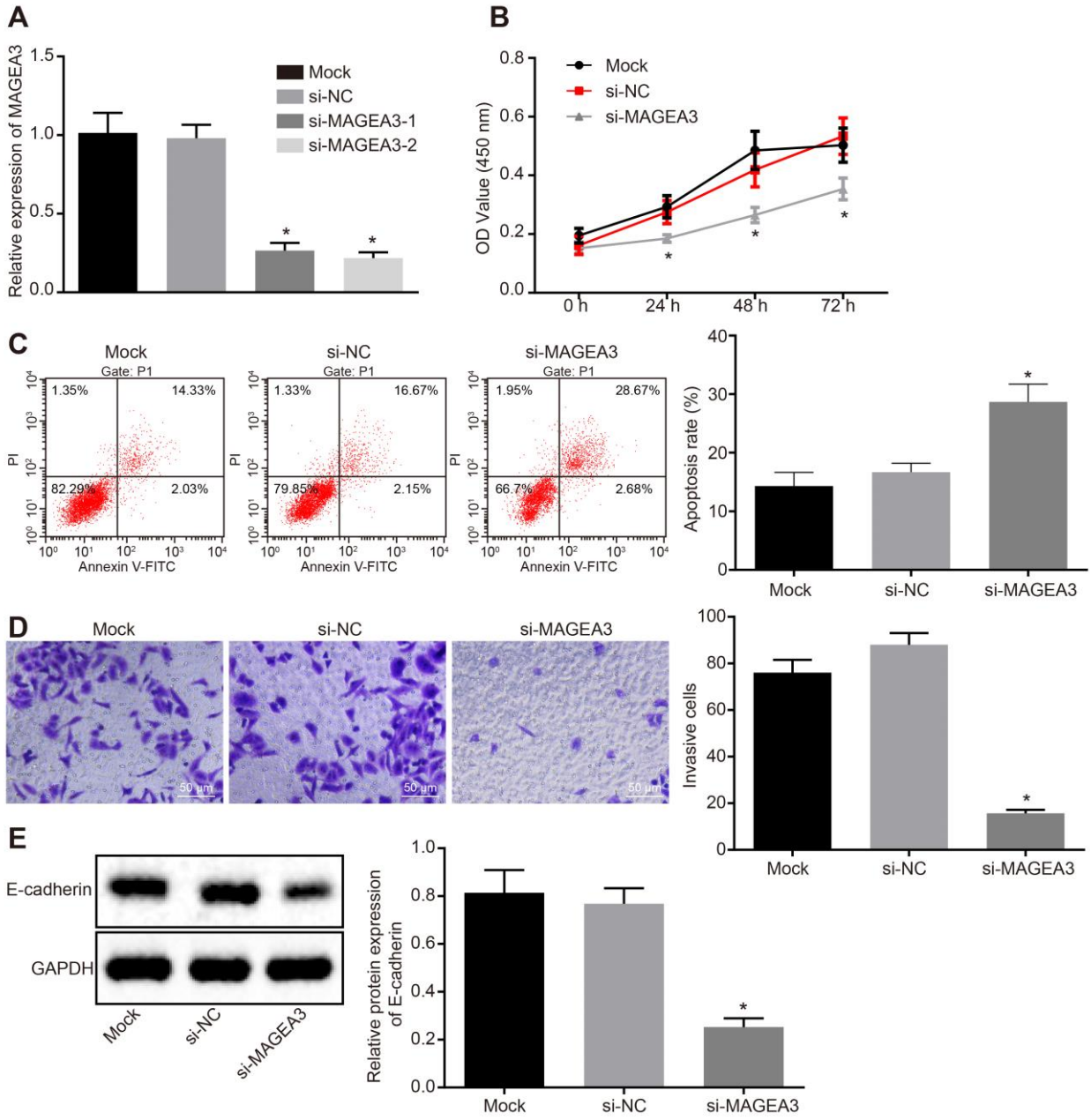

Supplementary Figure 1. Depleted MAGEA3 represses the proliferation and invasion but potentiates the apoptosis of Huh7 cells. A, transfection efficiency of siRNAs targeting MAGEA3 (si-MAGEA3-1, si-MAGEA3-2, si-MAGEA3-3) in Huh7 cells determined using RT-qPCR; B-D, viability (B), apoptosis (C) and invasion (× 200; D) of Huh7 cells in response to MAGEA3 depletion, as measured using MTT assay, flow cytometry and Transwell assay, respectively; E, protein expression of E-cadherin in Huh7 cells in response to MAGEA3 depletion measured using Western blot analysis. Measurement data were expressed as mean ± standard deviation. Data in panel B were analyzed using repeated-measures ANOVA along with Tuckey's post hoc test and data among groups in other panels were compared using one-way NAOVA together with Tuckey's

post hoc test. The experiment was repeated three times. *$p < 0.05$ vs. mock- or si-NC-transfected Huh7 cells.

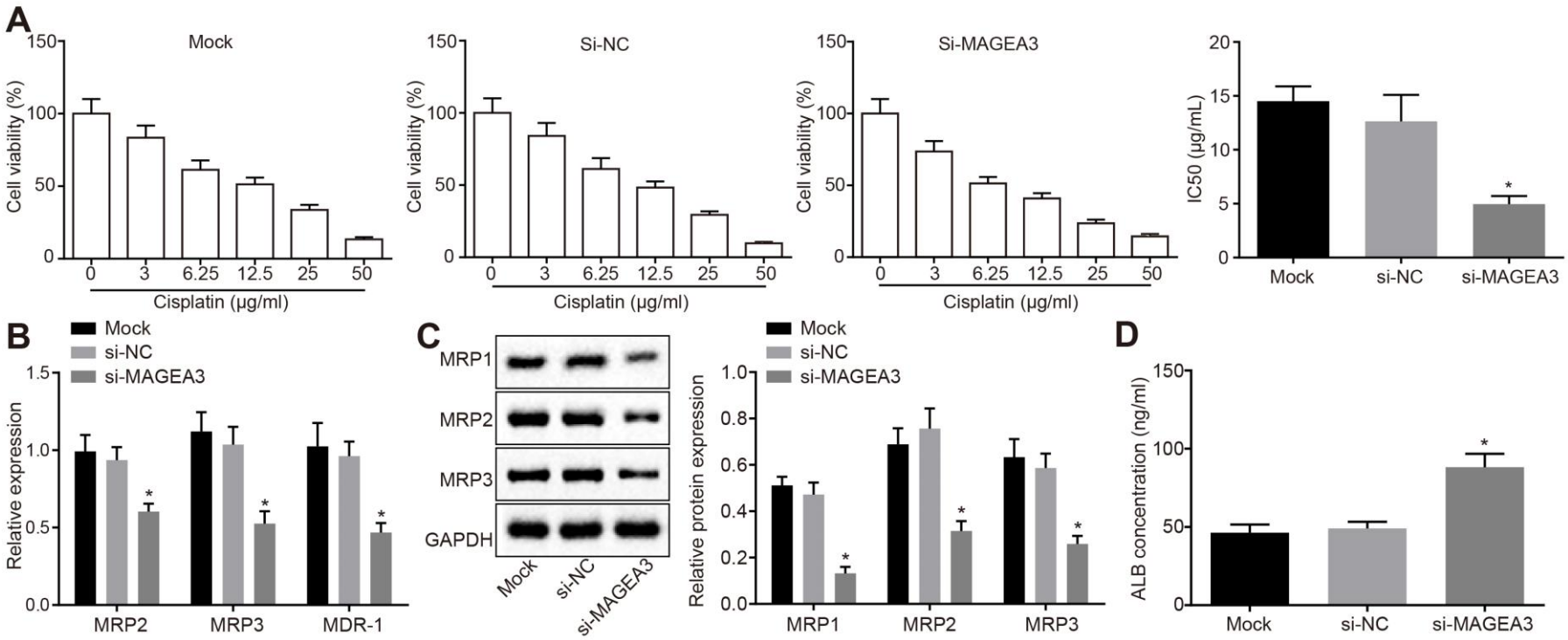

Supplementary Figure 2. MAGEA3 silencing reduces chemoresistance of Huh7 cells to cisplatin. A, CCK-8 assay showing viability and the IC_{50} of Huh7 cells transfected with mock, si-NC or si-MAGEA3 upon treatment with cisplatin at different concentrations; B, the mRNA levels of MRP2, MRP3 and MDR1 in Huh7 cells following silencing of MAGEA3 determined by RT-qPCR; C, the protein levels of MRP2, MRP3, and MDR1 in Huh7 cells transfected with si-MAGEA3 measured by Western blot analysis. D, ALB content in the supernatant of Huh7 cells in response to si-MAGEA3 transfection detected by ELISA. Measurement data were expressed as mean ± standard deviation. The comparisons among multiple groups were assessed with one-way ANOVA, followed by Tukey's post hoc test. Each experiment was repeated three times. * $p < 0.05$ *vs.* the mock- or si-NC-transfected Huh7 cells.

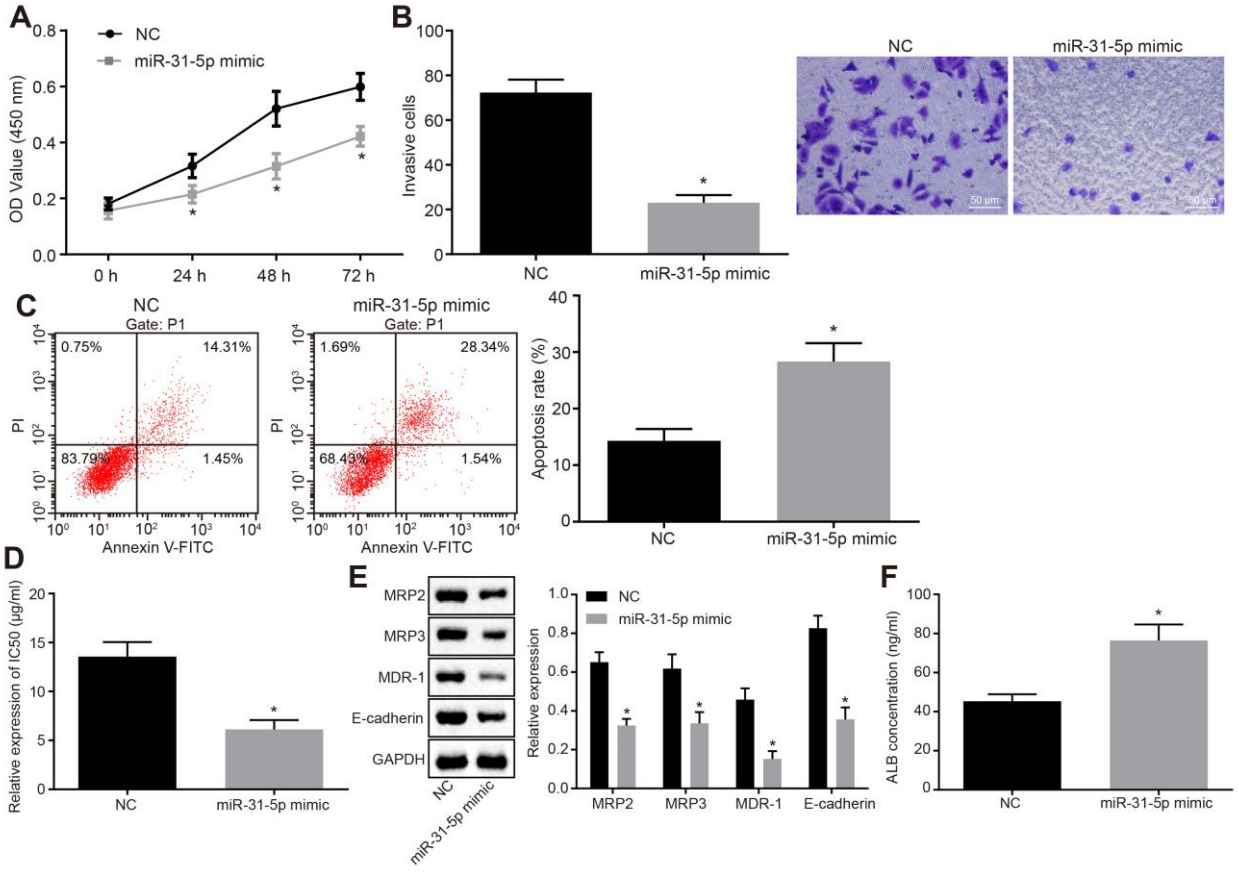

Supplementary Figure 3. miR-31-5p dampens Huh7 cell proliferation and reduces chemoresistance to cisplatin. A-C, viability (A), invasion (×200; B) and cisplatin-induced apoptosis (C) of Huh7 cells in response to miR-31-5p mimic transfection using MTT assay, Transwell assay and flow cytometry, respectively; D, IC_{50} value of Huh7 cells in response to miR-31-5p mimic transfection; E, protein expression of MRP2, MRP3, MDR-1, and E-cadherin in Huh7 cells in response to miR-31-5p mimic transfection measured by Western blot analysis; F, content of ALB in the supernatant of Huh7 cells in response to miR-31-5p mimic transfection detected using ELISA. Measurement data were expressed as mean ± standard deviation. The comparison between two groups was analyzed by independent sample *t*-test and the comparisons among multiple groups by one-way ANOVA, followed by Tukey's post hoc test. Data in panel C were analyzed using repeated-measures ANOVA with Tuckey's post hoc test. Each experiment was repeated three times. * $p < 0.05$ vs. NC-transfected Huh7 cells.

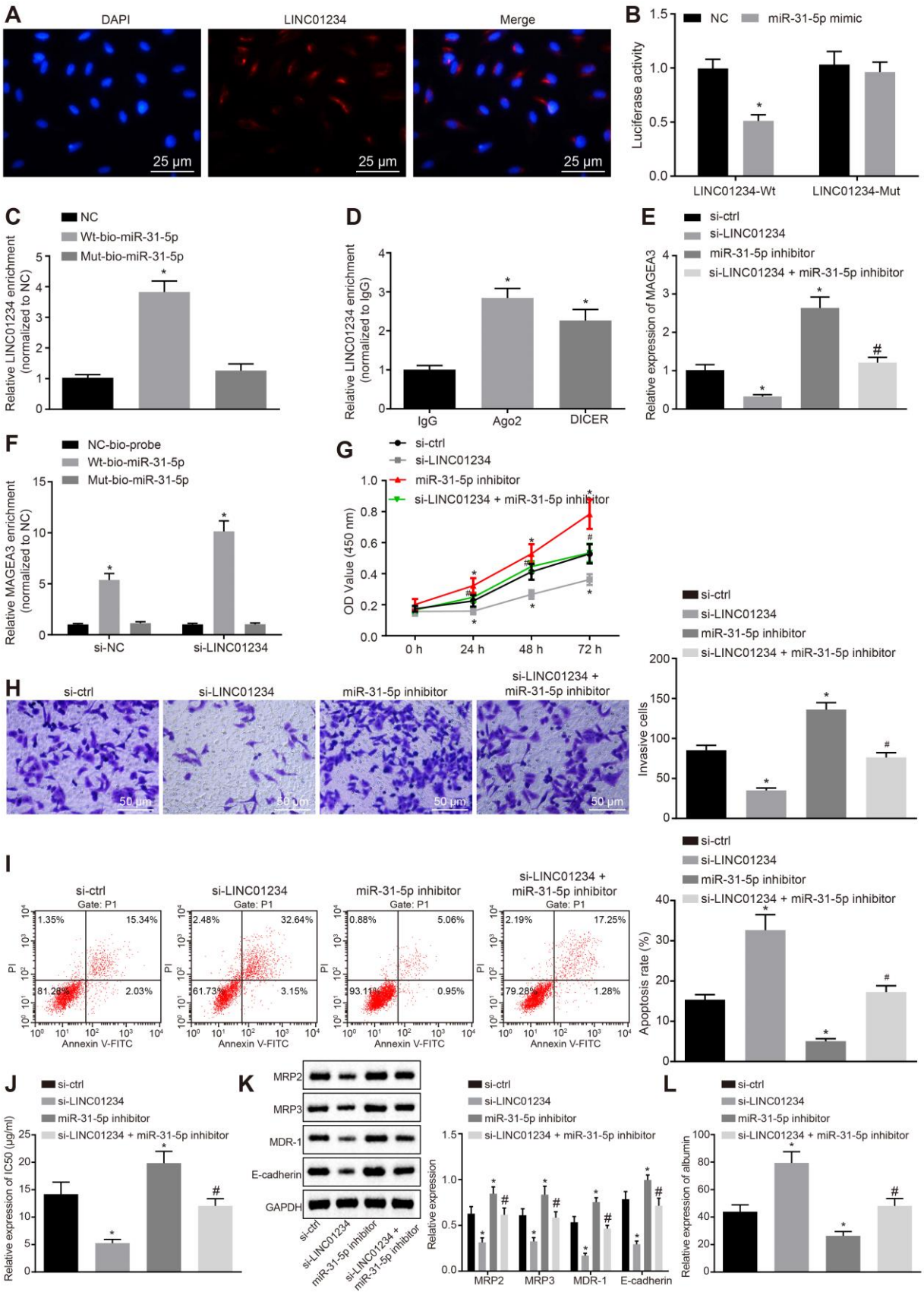

Supplementary Figure 4. Reduction of LINC01234, results in suppression of HCC progression *via* miR-31-5p-mediated inhibition of MAGEA3. A, the subcellular localization of LINC01234 in Huh7 cells detected using FISH (× 400); B, the luciferase activity of LINC01234 in Huh7 cells

upon miR-31-5p mimic transfection detected by dual-luciferase reporter gene assay; C, the binding between LINC01234 and miR-31-5p in Huh7 cells detected by RNA pull-down assay; D, the binding between LINC01234 and Ago2 or DICER in Huh7 cells detected by RIP assay; E, MAGEA3 expression in Huh7 cells measured using RT-qPCR; F, binding of miR-31-5p to MAGEA3 in Huh7 cells detected using RNA pull-down; G-I, the viability (G), invasion (× 200; H) and cisplatin-induced apoptosis (I) of Huh7 cells upon silence of LINC01234 and/or miR-31-5p evaluated by MTT assay, Transwell assay (× 200) and flow cytometry, respectively; J, IC_{50} value of Huh7 cells upon silence of LINC01234 and/or miR-31-5p; K, protein expression of MRP2, MRP3, MDR-1, and E-cadherin in Huh7 cells determined using Western blot analysis; L, content of ALB in the supernatant of Huh7 cells detected by ELISA. Measurement data were expressed as mean ± standard deviation. Differences among groups at different points of time were assessed with repeated-measures ANOVA. The comparison between two groups was analyzed by independent sample *t*-test and the comparisons among multiple groups by one-way ANOVA, followed by Tukey's post hoc test. Each experiment was repeated three times. **p* < 0.05 *vs.* the IgG immunoprecipitates or the NC- or si-ctrl-transfected cells; #*p* < 0.05 *vs.* the si-LINC01234-transfected cells.